Thermoreflectance Imaging of Superlattice Micro Refrigerators

James Christofferson, Daryoosh Vashaee, Ali Shakouri*
Jack Baskin School of Engineering, University of California, Santa Cruz, CA 95064

Philip Melese
SRI International, Menlo Park, CA 94025

Xiaofeng Fan, Gehong Zeng, Chris Labounty, and John E. Bowers
Electrical and Computer Engineering, University of California, Santa Barbara, CA 93106

Edward T. Croke III
HRL Laboratories, LLC

* Tel. (831) 459-3821, FAX (831) 459-4829, ali@cse.ucsc.edu

Abstract

High resolution thermal images of operating micro refrigerators are presented. Using the thermoreflectance method and a high dynamic range PIN array camera, thermal images with 50mK thermal resolution and high spatial resolution are presented. This general method can be applied to any operating semiconductors, and can be used as a tool for identifying fabrication failures. With further optimization of the experimental setup, we expect to achieve sub-micron spatial resolution thermal images.

Introduction

For various applications in optoelectronic or high power electronic devices, it is useful to control the temperature on a microscopic scale. For example, semiconductor lasers used in wavelength division multiplexed fiber optics communication systems require less than a degree centigrade variation in their operating temperature in order to have stable wavelength and output power. The traditional thermoelectric effect that can provide cooling at the interface between two materials can be enhanced using thermionic emission in superlattice barriers [1,2]. By integrating these heterostructure integrated thermionic(HIT) micro coolers with lasers, and other opto-electronic devices, we can have active temperature control on a small scale thus improving the reliability of thermally sensitive systems. Room temperature thermocouple measurements show 4 degrees centigrade of cooling on the surface of the cooler. However, since the size of the micro-coolers can be smaller then the thermocouple, and the measurement is effected by the thermal mass of the thermocouple, non-contact high-resolution methods are preferred for obtaining device performance.

Thermoreflectance techniques

Many experiments have used the thermoreflectance method for thermal measurements on a microscopic scale. In particular experiments by Goodson[3], Quintard[4] and Claeys[5] have shown good results on metal trace experiments and also several experiments by Mansares[6] and Batista[7] have shown thermal imaging with a scanning method. The thermoreflectance technique exploits the change in the reflection coefficient of material with temperature. Using visible wavelength one can achieve submicron spatial resolution.

It is known that the reflection coefficient has a small linear dependence on temperature. The normalized change in reflection per unit temperature is called the thermoreflectance constant and is denoted by C_{th}.

$$C_{th} = (1/R)(dR/dT)$$

Cth is 1.5e-4 for silicon and around 1e-5 for metals.

Because of the small temperature dependence of the reflection coefficient we must modulate the temperature and use heterodyne filtering. We excite the sample with a current pulse, and as long as the excitation period is long enough for the device to reach thermal equilibrium, the magnitude of the flicker seen at the detector at the excitation of the frequency is proportional to the change in temperature.

Let the reflection coefficient of the sample be the initial reflection coefficient at ambient, R_0, plus the change from a change in temperature.

$$R(T)=R_0 + dR/dT * \Delta T$$

Let P_{ref} be the power reflected of the sample, and acquired by the photo detector, or pixel and P_{in} be the optical power incident on the sample.

$$P_{ref} = P_{in} * (R_0 + dR/dT *\Delta T)$$

$$P_{ref}= P_{in}R_0 + P_{in}\, dR/dT * \Delta T$$

Let us assume that ΔT is periodic at some excitation frequency ω. Let P_ω be the power at the excitation frequency that we recover through heterodyne filtering.

Report Documentation Page

Form Approved
OMB No. 0704-0188

1. REPORT DATE	2. REPORT TYPE	3. DATES COVERED
2006		**00-00-2006 to 00-00-2006**

4. TITLE AND SUBTITLE	5a. CONTRACT NUMBER
Thermoreflectance Imaging of Superlattice Micro Refrigerators	5b. GRANT NUMBER
	5c. PROGRAM ELEMENT NUMBER
6. AUTHOR(S)	5d. PROJECT NUMBER
	5e. TASK NUMBER
	5f. WORK UNIT NUMBER
7. PERFORMING ORGANIZATION NAME(S) AND ADDRESS(ES) **Baskin School of Engineering,University of California,Santa Cruz,CA,95064**	8. PERFORMING ORGANIZATION REPORT NUMBER
9. SPONSORING/MONITORING AGENCY NAME(S) AND ADDRESS(ES)	10. SPONSOR/MONITOR'S ACRONYM(S)
	11. SPONSOR/MONITOR'S REPORT NUMBER(S)

12. DISTRIBUTION/AVAILABILITY STATEMENT
Approved for public release; distribution unlimited

13. SUPPLEMENTARY NOTES
The original document contains color images.

14. ABSTRACT

15. SUBJECT TERMS

16. SECURITY CLASSIFICATION OF:			17. LIMITATION OF ABSTRACT	18. NUMBER OF PAGES	19a. NAME OF RESPONSIBLE PERSON
a. REPORT	b. ABSTRACT	c. THIS PAGE			
unclassified	**unclassified**	**unclassified**		**6**	

$P_\omega = P_{in} * dR/dT * \Delta T$

And recalling the definition of the thermoreflectance constant

$C_{th} = 1/R_0 * dR/dT$

Thus the change in temperature is

$\Delta T = P_\omega/(P_{in}*R_0*C_{th})$

But $P_{in}*R_0$ is simply the unmodulated, DC reflectivity of the sample. Therefore, the experimentally obtained change in temperature is the lock-in signal divided by the normalization, which is the DC magnitude, times the thermoreflectance constant.

The thermal resolution depends on several factors; how much incident light is reflected off the sample, the value of C_{th}, how large is the area we are measuring, and also the bandwidth window resulting from the heterodyne filtering. The amount of thermal signal compared to the fundamental shot and Johnson noise, dictates the overall thermal resolution. In practice, for an area corresponding to $10\mu m^2$ of the device, we have about 1μA photocurrent, of which only 10pA is the modulated thermoreflectance signal. Thus for good signal to noise, we need to perform a 30 second FFT, corresponding to a .033Hz window.

Experimental Setup

The simple experimental setup is shown in figure 1. A white light from a fiber-optic illuminator is reflected off the sample, and the enlarged image of the device is collected by the camera.

To generate a thermal image, the amount of thermoreflectance signal is normalized to the total amount of light on the surface of the device. This means our thermal camera must have dynamic range on the order of the thermoreflectance constant. Because of this, a standard CCD cannot be used. To capture thermal images, we need a camera with high dynamic range and enough sensitivity to capture the small thermoreflectance signal. In fact a few experiments have tried to use a traditional CCD[8,9] for capturing thermal images, but such experiments were only sensitive to changes of 10's of degrees.

At SRI International a camera has been developed that can be used to capture thermal images. Each pixel of the SRI camera receives different gain for the AC and DC signal, then is heterodyne filtered with a fast Fourier transform(FFT). The camera is based on the Hamamatsu 16x16 PIN array detector.

The main advantage comparing to conventional infrared cameras is the improved spatial resolution. Typical HgCdTe-based cameras have a diffraction limited spatial resolution of 3-5 microns, while visible wavelength thermoreflectance imaging can give submicron resolution. On the other hand, the cooling or heating over small areas can be measured accurately without the effect of background radiation. For example a very low ambient temperatures, there is not enough blackbody radiation to measure the device performance.

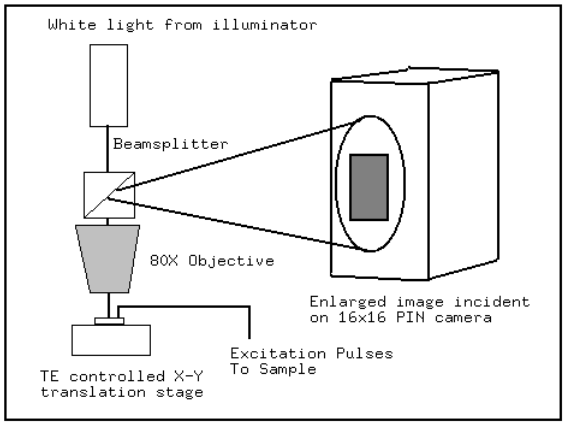

Figure1: Experimental Setup.

Processing the Images

Generating thermal images from the raw data, consists of normalization, correcting for different C_{th} values, and determining the heating and cooling points.

Normalization consists of simply accounting for the total amount of light that is reflected and can be accomplished by simply dividing the thermoreflectance image, by the DC, or normalization image. This should also account for variations in responsivity at different pixels of the camera.

Next, different reflection surfaces must be accounted for different thermoreflectance constants. Each material has a different C_{th} and therefore to obtain an accurate thermal image, different values are assigned to different reflection surfaces. In the micro-refrigerator images, there is only the gold reflection surface, and also silicon. This can almost be corrected automatically, as the histogram of the normalization image is bi-modal, due to a lower overall reflectivity of silicon.

Finally we must determine which points in the image are heating and cooling. From the FFT we know the overall magnitude of the thermal signal, but we must look at the phase image to know if the thermal change is positive or negative. This is exacerbated by the fact that our camera introduces a slight phase difference per pixel because the channels are not read exactly in parallel. This operation can be automated, provided that the user input the dominant phase.

Experimental Results

The geometry of the micro cooler samples is show in figure 2. Images of a 10x10micron operating micro refrigerator are presented. Figure 3 shows the normalization image of the cooler. The image is interpolated from the 16x16 pixels of the SRI camera. Figure 4 shows the thermal image and a little more then 3 degrees centigrade of cooling on the surface of the cooler. Figure 5 shows a countour plot of the thermal image.

In figure 6 we see an image of a larger micro cooler and a current probe on top of the device. The latest micro-coolers have the geometry as shown in figure 2, with a long contact layer so that the heating from the current probe would not effect the cooling on the surface. Previous generations of the cooler required that the current probe sit directly on top of

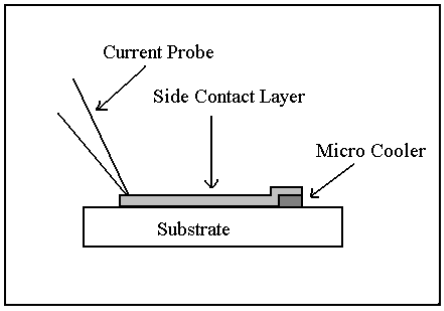

Figure 2: Geometry of Micro Refrigerator Samples

the cooler. Figure 6 shows the 100x180 micron micro refrigerator and the (out of focus) current probe in the foreground. As expected, in the thermal image, figure 7, there is excessive heating caused by the current probe. What is a surprise, however, is that there is close to 4 degrees of cooling very near the probe which is caused by the high current density in that area. Previous thermocouple measurements of this device measured less then 2 degrees of cooling, which is what we see over most of the device after the current has spread out. Figure 8 shows a cross section across the device depicting the hot and cool regions of the micro refrigerator. This image is not exactly correct, because we would have determine C_{th} for the material of the current probe. Since we are not that concerned with the exact heating caused by the probe, C_{th} for the probe is taken as the same as gold.

Identifying Fabrication Failures

Another useful aspect of the thermal imaging camera is that it can be used to identify fabrication failures. Figure 9 shows a CCD image of a 20x20micron micro-cooler. The normalization image is shown in figure 10. Two different thermal images of 20x20 operating micro coolers are presented at the same operating current. Figure 11 shows a well fabricated device and a nice cooling distribution across the device, while in figure 12 we see a device that has excessive heating at the boundary from the contact layer to the micro cooler. This has been identified as a error in the deposition of the contact layer. This failure could not be observed by looking at the CCD images. The cross-section of the correctly fabricated, and the poorly fabricated device are shown in figure 13.

Conclusion

Thermoreflectance imaging is used to determine the performance of superlattice refrigerators, and can also identify fabrication failures. This method can be applied to other active devices and integrated circuits, and because we use visible light the spatial resolution can be better then typical 3 micron IR cameras. With further optimization of the light source and camera, we expect to improve the thermal resolution and achieve real time sub-micron thermal images.

Acknowledgements

We would like to thank Ed Croke for the molecular beam epitaxy growth and also Xiofeng Fan and Gehong Zheng for the fabrication of the cooler samples used in this experiment. This work was funded by the Packard Foundation and DARPA Heretic program. Support for this project was provided by the Department of the Army, Army research Office, and the content of information does not reflect the position of the federal government, and no official endorsement should be inferred.

Refrences

1.Ali Shakouri and John E. Bowers, "Heterostructure Integrated Thermionic Coolers", Applied Physics Letters, 71(9), pp. 1234-1236, September 1997.

2. Gehong Zeng; Shakouri, A.; Bounty, C.L.; Robinson, G.; Croke, E.;Abraham, P.; Xiafeng Fan; Reese, H.; Bowers, J.E. "SiGe micro-cooler,"Electronics Letters, vol.35 (24), 25:2146-7, Nov. 1999.

3. K.E. Goodson and Y.S. Ju, "Short-time-scale thermal mapping of microdevices using a scanning thermoreflectance technique," *Trans. of the ASME*, p.306-313, May 1998.

4. Quintard, Dilhaire, Phan, and Claeys. "Temperature measurement of metal lines under current stress by high resolution laser probing," *IEEE Trans. on Instrumentation and Measurement*, p.69-74, Feb 1999.

5. T Phan, S Dilhaire, V Quintard, W Claeys, and J Batsale. "Thermoreflectance measurements of transient temperature upon integrated circuits: application to thermal conductivity identification,"*Microelectronics Journal*, 29:181-190, 1998.

6. A Mansanares, D Fournier, A Boccara. " Temperature measurements of telecommunication lasers on a micrometre scale", *Electronics Letters*, 29(23):2045-2047, 1993.

7. J. Batista, A Mansanares, EC DaSilva, M Pimentel, N Januzzi, D Fournier. "Subsurface microscopy of biased metal oxide semiconductor field effect transistor structures: photothermal and electroreflectance images," *Senors and Actuators A*, 71:40-45, 1998.

8. T Spirig, P Seitz, O Vietze, and F. Heitger. "The lock in ccd, two dimensional synchroneous detection of light," *IEEE Journal of Quantum Electronics*, p.1705-1708, Sept. 1995.

9. S Grauby, S Hole and D Fournier. "High resolution photothermal imaging of high frequency using visible charge couple device camera associated with multichannel lock-in scheme," *Review of Scientific Instruments.* P.3603-3608, Sept.1999.

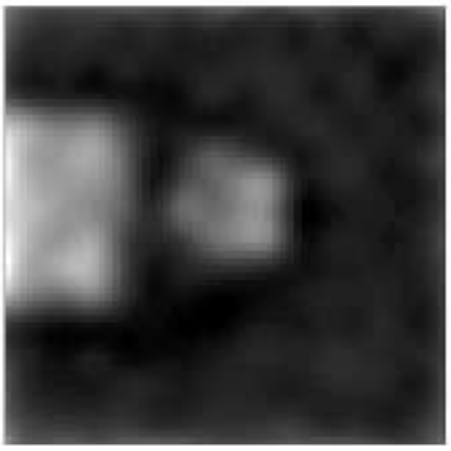

Figure 3: Normalization image of 10x10 micron refrigerator from thermal camera

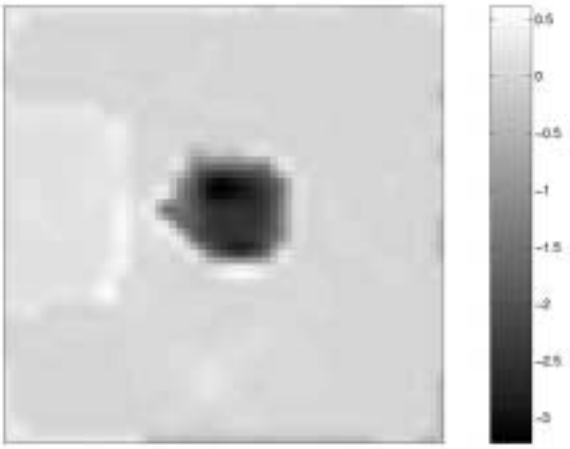

Figure 4: Thermal Image of 10x10 micron refrigerator

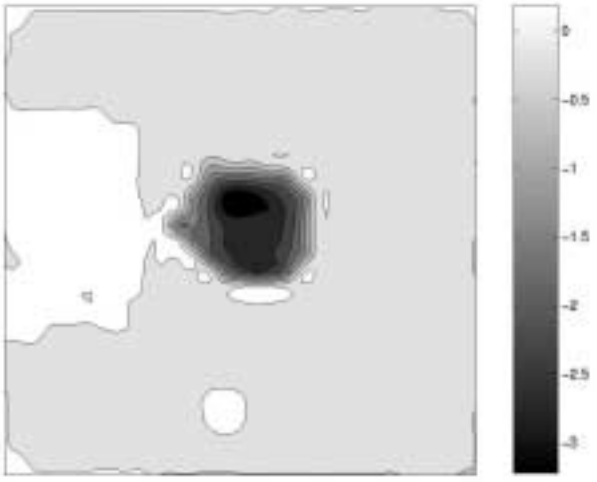

Figure 5: Contour Plot of Thermal Image

Figure 6: Normalization image from thermal camera showing current probe on top of micro refrigerator

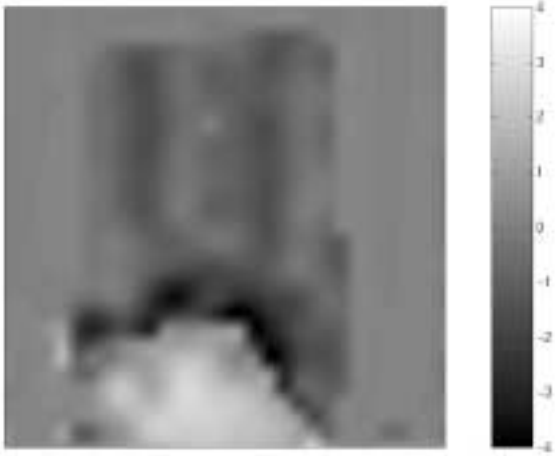

Figure 7: Thermal Image showing heating at current probe and cooling on cooler surface.

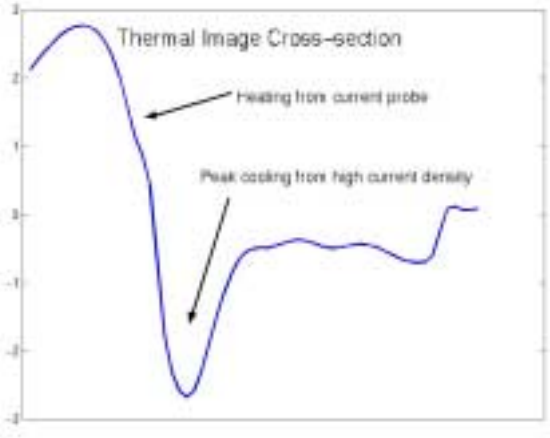

Figure 8: Cross-section of thermal image

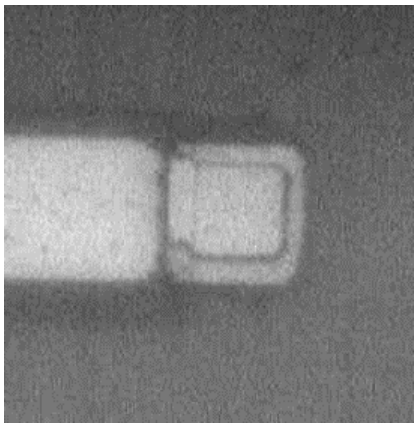

Figure 9: CCD Image of 20x20 micron Micro Refrigerator.

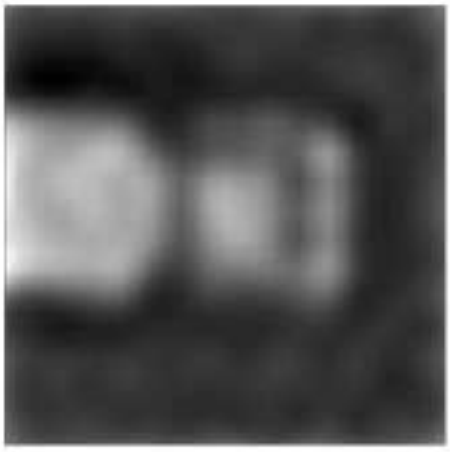

Figure 10: Normalization image seen through the thermal camera.

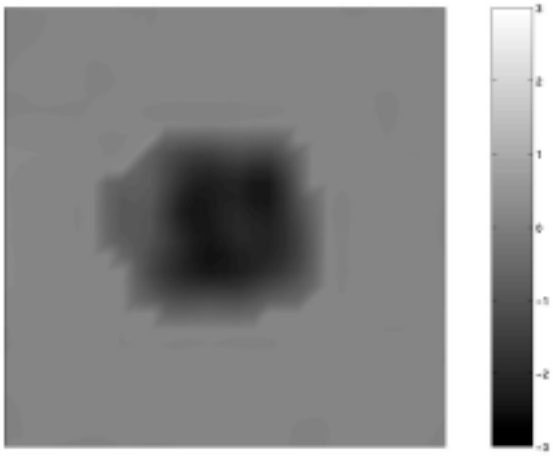

Figure 11: Good Cooling Distribution on well fabricated 20x20 micron device.

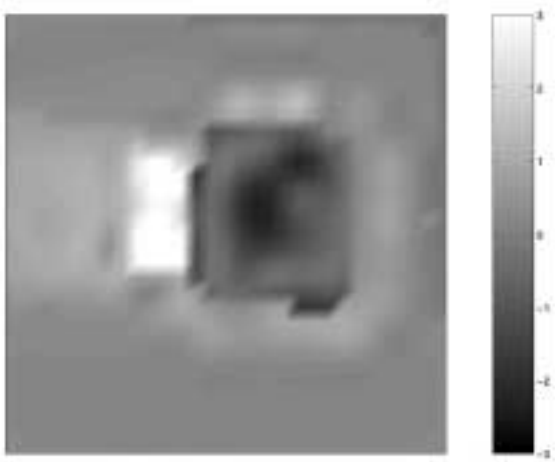

Figure 12: Excessive heating at the boundry from fabrication error.

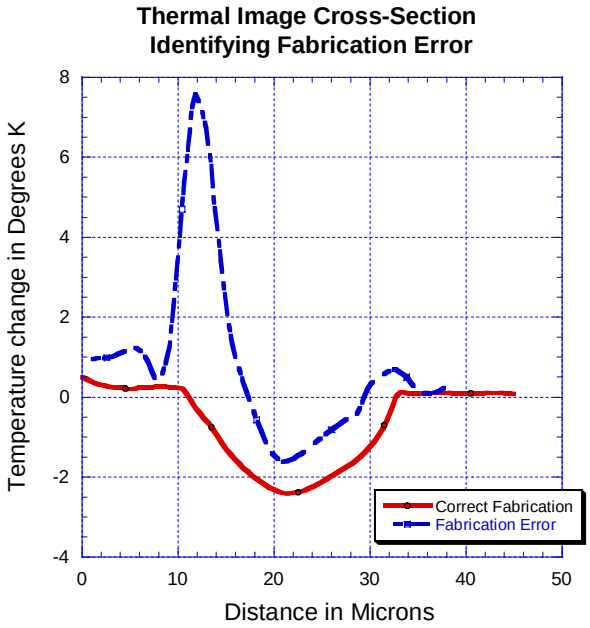

Figure 13: Cross-section plot comparing two 20x20 micron devices.